v. 14, n. 3, p. 81-89, 2025 ISSN 2237-9223



**DOI:** <a href="http://dx.doi.org/10.15260/rbc.v14i3.936">http://dx.doi.org/10.15260/rbc.v14i3.936</a>

# Estimating Vehicle Speed in Forensic Traffic Accident Analysis: An R/Shiny Implementation of the Monte Carlo Method and Cross-Ratio

C. R. De Musis<sup>a\*</sup>, I. De Musis<sup>b</sup>, T. J. Gross<sup>a</sup>, B. S. De Martinis<sup>c</sup>

<sup>a</sup> Perícia Oficial e Identificação Técnica do Estado de Mato Grosso

<sup>b</sup> Secretaria de Estado de Saúde do Estado de Mato Grosso

<sup>c</sup> Departamento de Química da Faculdade de Filosofia, Ciências e Letras de Ribeirão Preto da Universidade de São Paulo

\*Endereço de e-mail para correspondência: carlodemusis@politec.mt.gov.br. Tel.: +55-65-992625221.

Recebido em 02/01/2025; Revisado em 28/07/2025; Aceito em 23/08/2025

#### Resumo

Este estudo apresenta uma abordagem para estimar velocidades em análises forenses de acidentes de trânsito, combinando o método de Monte Carlo com estimativas fotogramétricas baseadas na razão cruzada. Para sua aplicação prática, foi desenvolvido um software na linguagem R, utilizando a biblioteca Shiny, que oferece uma interface interativa via WEB. A metodologia foi testada em um estudo de caso envolvendo um veículo em escala reduzida, onde as velocidades estimadas foram comparadas às obtidas com o software Amped Five, uma referência do mercado, que utiliza fotogrametria bidimensional. A análise estatística, realizada com o teste de Wilcoxon, não detectou diferenças significativas entre os métodos (p > 5%), dispondo, assim, a metodologia como uma alternativa viável para investigações forenses.

Palavras-Chave: Razão cruzada complexa, geometria projetiva, análise de incertezas.

# Abstract

This study presents an approach to estimate speeds in forensic traffic accident analyses, combining the Monte Carlo method with photogrammetric estimates based on cross-ratio. For practical application, a new software was developed in the R programming language using the Shiny library, providing an interactive web interface. The methodology was tested in a case study involving a scaled-down vehicle, where the estimated speeds were compared to those obtained with the Amped Five software, a market reference that uses two-dimensional photogrammetry. Statistical analysis, conducted with the Wilcoxon test, did not detect significant differences between the methods (p > 5%), thereby suggesting the methodology as a viable alternative for forensic investigations.

Keywords: Complex cross-ratio, projective geometry, uncertainty analysis.

## 1. Introduction

Traffic accidents represent a severe global public health concern, ranking among the leading causes of death and sequelae in the young and economically active population. According to Santos and Araujo [1], traffic accidents primarily affect young people and constitute a significant public health issue in the state of Roraima, Brazil. Zanon and Brisotto [2] noted that human factors significantly impact the causes and consequences of traffic accidents, particularly concerning drivers' conduct and behavior, with a focus on inattention and overconfidence. Massaú and Rosa [3] alert that the prevention of traffic accidents

represents an important act of public health management, both by reducing direct expenses in the Brazilian Unified Health System (SUS) and by decreasing indirect costs related to the social security system, the victims, their families and the economic system at large. In a similar argument, Ramos, Barreto and Miguel [4] state that accident reconstruction plays a fundamental role in investigating the causes and dynamics of these events, as well as contributing to the prevention of new accidents.

The technical and methodological proficiency involved in accident reconstruction, although initially seemingly distant from the social sciences, finds a conceptual bridge in the reflections made by Arendt [5] on fundamental human activities and their implications for life in society and politics. The author develops a conceptual framework to understand the nature and value of these activities, arguing that they are essential to comprehend the human condition in its entirety.

In this context, criminalistics, which employs reconstruction methods to elucidate the circumstances of criminal events, can be seen as an example of Arendtian "work". According to Arendt, work is the activity corresponding to the artificiality of human existence, producing an "artificial" world of things, distinctly different from the natural environment, providing some permanence and durability to the futility of mortal life and the ephemeral nature of human time.

Thus, by creating detailed reconstructions of accidents, criminalistics engages in this process of manufacturing an artificial world that aids in the narrative and comprehension of complex events. This Arendtian perspective allows considerations on the value and meaning of this practice, situating it within a broader conceptual framework of fundamental activities that condition human existence.

On the other hand, criminology, with its focus on the study of crime, its causes and ways to prevent it, engages in the spheres of "labor" and "action". Through labor, it seeks to maintain social life through the prevention and comprehension of crime, while action manifests in public debate and political and social interventions aimed at addressing and preventing crime.

Criminalistics and criminology are complementary and essential in understanding and responding to crime, interlinking through the analytic categories proposed by Arendt. Applying this vision to the reconstruction of traffic accidents highlights the role of forensic sciences in this context, where reconstructing an accident using scientific methods, such as the Monte Carlo method and cross-ratio, would be a paradigmatic example of work in the Arendtian sense, resulting not only in the development of a tool that, in principle, assists in clarifying the factual truth about the event, but also provides information for criminology. Operating in the sphere of "action", criminology seeks to understand the root causes of accidents and to formulate more effective preventive strategies and public policies. Therefore, the synergy between the "work" performed in criminalistics and the "action" in criminology, through the elucidation of truth, is essential to address the complex challenges presented to contemporary society.

As a segment within the realm of "work", this article presents a method for the reconstruction of traffic accidents, exploring the use of the Monte Carlo Method (MCM) in conjunction with the concept of cross-ratio, an invariant under specific conditions, and projective geometry to directly determine vehicle speeds based on video recordings. This approach offers an alternative method for analyzing such incidents, providing resources

for the development of prevention strategies and the reduction of the negative impacts of traffic accidents on public health and on society as a whole.

The reconstruction of traffic accidents seeks, through the evidence present at the scene and physicalmathematical modeling, to reproduce the sequence of events and parameters involved in the collision, such as speeds, trajectories, and actions of the drivers. However, this process involves various uncertainties associated with the stochastic nature of the variables used. To deal with those uncertainties, statistical techniques such as the MCM can be employed. This technique performs simulations based on the stochastic modeling of input variables, allowing for the propagation of uncertainties and obtaining probability distributions of the parameters of interest in the Meanwhile, reconstruction [6]. the photogrammetric estimation procedure proposed by Wong et al. [7] allows, when applicable, for the determination of vehicle speeds directly from video images, without the need for external references.

In this article, we aim to present a software designed to assist in the application of the Monte Carlo and cross-ratio methods in the task of traffic accident reconstruction. We will begin with an exploration of the theoretical foundations that underpin the reconstruction process, followed by a detailed description of the Monte Carlo method, including practical examples of implementation for uncertainty propagation. Subsequently, the cross-ratio technique will be examined as a procedure for estimating vehicle speed from images. The discussion will be complemented by a reduced-scale experiment, which will serve to illustrate and evaluate the efficacy of the joint application of these techniques, culminating in a reflection on future prospects and challenges inherent in the field of traffic accident reconstruction.

## 2. METHODOLOGY

#### 2.1. Cross-ratio

Each image frame captured by a recording device constitutes a two-dimensional representation of a three-dimensional space. Every position in the three-dimensional real world that is captured within a frame is mapped to a two-dimensional point on the image plane. The mapping, or transformation, from three-dimensional space to two-dimensional space follows the principles of projective geometry. Figure 1 illustrates the mapping of a line A'B'AB in the three-dimensional real world to a two-dimensional space in the image frame, namely line N'M'NM.

Based on Wong et al. [7], the concept of cross-ratio was adopted to establish proportional relationships between measurements in a geometric context, facilitating the understanding of how dimensions in different spaces or systems relate to each other. Cross-ratio is a foundational

concept in projective geometry that allows us to compare the relationship between four collinear points in such a way that this relationship remains invariant under projection.

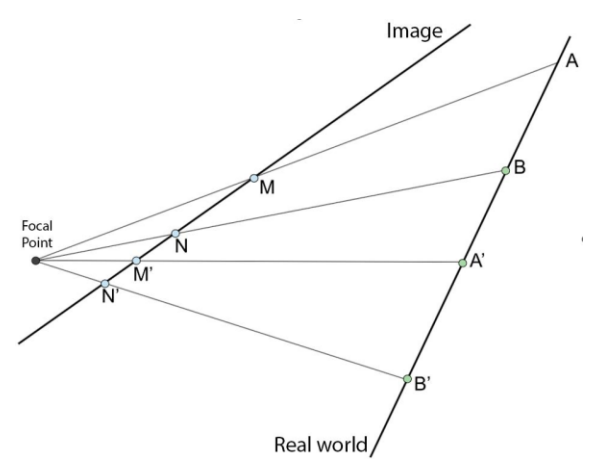


**Figure 1.** Schematic representation of a projective transformation from physical space to a two-dimensional image plane.

Mathematically, given a sequence of four collinear points, B', A', B and A, the cross-ratio between these points is defined as:

$$CR(B', A', B, A) = \frac{|B'B|}{|A'B|} \frac{|A'A|}{|B'A|}$$
 (1)

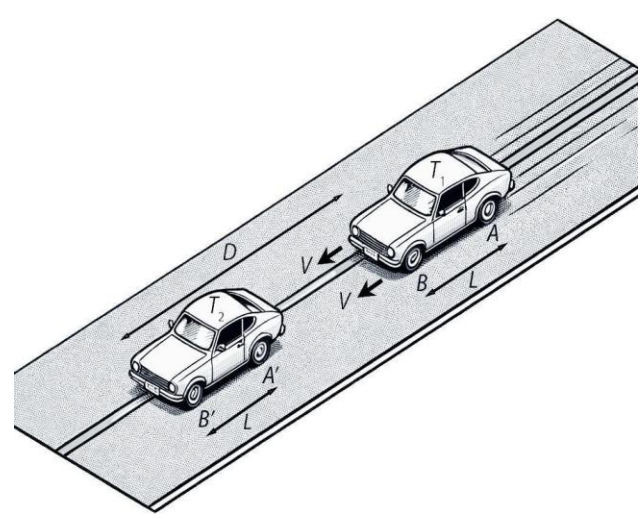


**Figure 2.** Schematic composition of two frames depicting the straight-line trajectory of a vehicle over a reference line at two instances,  $T_1$  and  $T_2$ , at a constant speed V.

$$CR(B', A', B, A) = CR(N', M', N, M)$$
(2)

The cross-ratio provides a method for comparing spatial relationships in such a way that they remain consistent even when viewed from different perspectives or through projective transformations. Figure 2 illustrates a vehicle moving along a straight-line trajectory at a uniform velocity V from time  $T_1$  to time  $T_2$ . (A', B') and (A, B) correspond to the positions of the front and rear wheels of the vehicle at times  $T_2$  and  $T_1$ , respectively. Here, D is the

distance traveled by the car and L is the wheelbase distance of the car. The cross-ratio of these points can be expressed in terms of D and L as follows:

$$|B'B| = D \tag{3}$$

$$|A'B| = D - L \tag{4}$$

$$|B'A| = D + L \tag{5}$$

$$|A'A| = D \tag{6}$$

$$CR(B', A', B, A) = \frac{D}{(D-L)} \frac{D}{(D+L)} = \frac{D^2}{D^2 - L^2}$$
 (7)

Rearranging and applying the functional form in D, representing the distance between A and A, we have:

$$D(A',A) = \pm \sqrt{\frac{CR(B',A',B,A)}{CR(B',A',B,A)-1}L^2}$$
 (8)

The cross-ratio CR(B',A',B,A) is an imaginary parameter in the three-dimensional real world, as the two pairs of points, B', A' and B, A, do not coexist simultaneously. However, if a car's movement is captured in a video, which is a sequence of temporally ordered images, it becomes possible to extract two image frames at  $T_1$  and  $T_2$  and construct a two-dimensional virtual image space. This space contains all the projected corresponding points from B' to A. From this two-dimensional virtual image space, the cross-ratio CR(B',A',B,A) can be indirectly determined.

Considering that the car was traveling in a straight path, the four points in the composite image are collinear. The trajectory N'M'NM in the virtual two-dimensional image space is the projected line of the straight trajectory B'A'BA in the real world. The pixel-to-pixel distances of MM', NM', MN' and NN' can be measured directly from the composite image to determine the cross-ratio CR(N',M',N,M).

# 2.2. Determination of vehicle speed

Due to the invariant property of the cross-ratio, the value of CR(N'M'NM) in the two-dimensional space of the image is equal to that obtained for CR(B',A',B,A) in the three-dimensional real world, substituting (2) into (8):

$$D(A', A) = \pm \sqrt{\frac{CR(N', M', N, M)}{CR(N', M', N, M) - 1} L^2}$$
(9)

From Equation (9), the distance traveled by the vehicle can be determined if the wheelbase is known. Therefore, the average scalar speed (V) between moments  $T_1$  and  $T_2$ ,

considering the spatial reference points A' and A, can be determined by:

$$V(A', A, T_2, T_1) = \frac{D(A'A)}{T_2 - T_1}$$
 (10)

# 2.3. Generalization to coplanar points

When considering points that are not necessarily collinear, such as in the case of a vehicle approaching the observer's point of view, the cross-ratio must be formulated using the coordinates of the points in the projective plane as complex numbers, known as the complex cross-ratio [8].

Equations 1 to 9 remain valid when extended to the complex domain. However, since the distance *D* becomes a complex number, it becomes necessary to consider its norm:

$$D_{metric}(A', A) = \left| \sqrt{\frac{RC(N', M', N, M)}{RC(N', M', N, M) - 1}} L^2 \right|$$
 (11)

Consequently, Equation 10 is revised to:

$$V(A', A, T_2, T_1) = \frac{D_{metric}(A'A)}{T_2 - T_1}$$
 (12)

These modifications enable the generalization of the method to scenarios involving coplanar points, ensuring mathematical consistency and applicability in a wider range of conditions.

The software implementation in this work reflected the theoretical extension by treating image points as complex coordinates and evaluating the complex cross-ratio, using its modulus to calculate distance and velocity.

# 2.4. Monte Carlo method

The Monte Carlo method is widely applied in various fields. In physics and chemistry, it is used in simulations of particle systems in high-energy physics, solid-state physics and nuclear physics [6].

In engineering, the method is applied in reliability and risk analysis of systems [9,10], radiation transportation simulations and dose calculations in medical physics [11] and fluid flow and heat transfer simulations [12].

In statistics and machine learning, the method is employed in parameter and uncertainty estimation in statistical models. Its applications include integration with Markov chain sampling in Bayesian inference and training of artificial neural networks [13, 14].

The mathematical foundation of the Monte Carlo method involves probability theory, statistics, and random sampling. Its core principle is based on the Law of Large Numbers, which states that the average of independent and

identically distributed observations converges to the expected value of the underlying distribution. The general process of the Monte Carlo method involves the following steps: (1) defining a domain of possible inputs for the problem; (2) generating random inputs from a probability distribution over the domain; (3) performing deterministic computations on the random inputs; and (4) aggregating the results of the individual computations into a final estimate [15].

Often, the estimation of vehicle speed through the cross-ratio method involves marking points on an image combining frames  $T_1$  and  $T_2$ . This process has intrinsic errors that can be statistically modeled. Assuming that the markings for the centers of each wheel are independent, convergent, and homoscedastic, they can be represented by bivariate Gaussian probability density functions N(X,Y), with X and Y being coordinates of the pixels in columns and rows, respectively.

In this case, these probability density functions and temporal markings are used to generate sets of cross-ratios, estimates of distance and speed, as well as their confidence intervals based on percentiles.

# 2.5. Evaluation of estimate quality

The assumption that the sample distribution of wheel markings adheres to a bivariate normal distribution can be evaluated for each wheel using a statistical procedure. The Doornik-Hansen test, developed to assess the quality of fit of a sample distribution to a bivariate normal distribution, is a multivariate extension of the univariate Shapiro-Wilk test that combines data transformations with matrix decomposition to create a goodness of fit test effective against most types of non-normality. It has good power and size properties and can be extended to higher dimensions [16].

Once the markings are validated, the next step is to estimate speed using the cross-ratio method. This procedure assumes that the markings are collinear, an assumption that can be evaluated through orthogonal regression, which accounts for random errors in both X and Y (Figure 3).

$$X = \xi + \delta, \qquad \delta \sim N(0, \sigma_{\delta}^2)$$
 (11)

$$Y = \eta + \varepsilon, \qquad \varepsilon \sim N(0, \sigma_{\varepsilon}^2)$$
 (12)

$$\eta = \beta_0 + \beta_1 \xi,\tag{13}$$

Here,  $\delta$  and  $\epsilon$  are independent random errors.  $\xi$  is assumed to be a random variable normally distributed with mean  $\mu$  and variance  $\tau^2$ , and independent from both random errors. Consequently, X and Y follow a bivariate normal distribution with mean and covariance matrix described as follows:

$$[XY] \sim N \left( \frac{[\mu \beta_0 + \beta_1 \mu],}{[\tau^2 + \sigma_\delta^2 \beta_1 \tau^2 \beta_1 \tau^2 \beta_1^2 \tau^2 + \sigma_\varepsilon^2]} \right) \quad (14)$$

The use of this model, which accounts for errors in both variables, offers a more balanced and potentially more accurate approach to estimating the relationship between pixel coordinates. This reasoning stems from the fact that, in the marking process, both variables are subject to random variation.

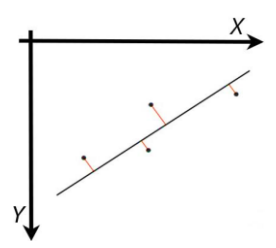


Figure 3. Schematic scatter plot of errors, in red, in an orthogonal regression for pixels located at reference points on the wheels.

However, it is important to note that the adherence of the bivariate distributions for each wheel does not guarantee, by itself, that the residuals of the model will also conform to this reference model. For this reason, an additional procedure was developed to assess the fit of the residuals from the orthogonal regression to the normal distribution, using the Shapiro-Wilk test.

The quality of the orthogonal regression fit was evaluated by the coefficient of determination (R<sup>2</sup>) and by the Akaike Information Criterion (AIC).

The coefficient of determination is a statistical measure that provides a direct interpretation of the model's effectiveness, indicating the proportion of variance in the dependent variable that is predictable based on the independent variable.

The Akaike Information Criterion is a useful measure for comparing different statistical models. It gauges each model's relative quality considering both its complexity (number of parameters) and its fit to the observed data [17]. Based on information theory, AIC directly measures the information lost when a model approximates the true process. Therefore, models with a lower AIC, and hence potentially more parsimonious in terms of complexity, would be closer to reality [18].

To validate the reference point estimates for wheelbase distance, a visual procedure based on the work of Gross [19] was developed. In the generated image, the pixel shades intersected by the final orthogonal regression line were analyzed, enabling the construction of a transect of distances along the regression relative to the grayscale values.

The wheels exhibit arrangements of shapes and colors in their components that define patterns with distinct points. These are prominent in the transects and typically define critical points, allowing for the validation of the reference coordinates used for measuring wheelbase difference, generally established as the center of the wheels.

#### 3. RESULTS AND DISCUSSION

## 3.1. Implementation

The application was developed using a set of open-source tools, composed of the programming language R [20], within the RStudio integrated development environment [21], and the Shiny library [22]. The latter is a tool that enables the development of web applications based on the Bootstrap framework [23]. The developed code is available for downloading in a public repository<sup>1</sup>.

Figures 4–8 reproduce the software's native output, generated in a Portuguese (Brazil) environment. The



Figure 4. Cropped, illustrative screenshot of the application's data-entry page and statistical outputs: orthogonal regression, coefficient of determination (R<sup>2</sup>), Akaike Information Criterion (AIC), and Doornik–Hansen normality test results.

<sup>&</sup>lt;sup>1</sup> Available at: https://github.com/demusis/fotogrametria.

interface language does not affect the algorithms, parameter values, or numerical results; it only reflects the locale of the development machine. To preserve fidelity and reproducibility, the screenshots are shown exactly as produced.

The application's interface includes two primary workspaces, accessible through a side menu on the left (Figure 4). The first workspace, labeled "Coordinates" ("Coordenadas"), corresponds to the environment for inputting the frame composition to be used as a reference in the cross-ratio calculation. In this area, a button has been provided for uploading an image containing the frame composition intended for analysis.

Once uploaded, the composition is displayed in the central region of the page. If the image's width in pixels exceeds the available area, scroll bars are activated on the right and bottom edges, allowing the complete visualization of the image. The system waits for the user to click on the composition, capturing the coordinates of each click and sequentially assigning them to the points of the cross-ratio.

The lower portion of Figure 4 displays key performance metrics: the orthogonal-regression equation,  $R^2$ , AIC, and the Doornik–Hansen test results, which evaluate whether the residuals follow a bivariate normal distribution ( $\alpha = 0.05$ ). A nonsignificant result is shown as 'NO' (Not Observed) for each wheel—thus 'NONONONO' when all four wheels pass the test.



**Figure 5.** Example of the adjusted orthogonal regression line with reference point markings overlaid on the composition presenting the analyzed car at two temporal markings generated by the application.

The Monte Carlo simulation's analytical and computational steps started with the system's definition through a numerical model. The inputs were the wheel markings on the frames for times  $T_1$  and  $T_2$ , time records of these frames, and the wheelbase of the analyzed car. The outputs, in turn, were the traveled distance and mean scalar speed.

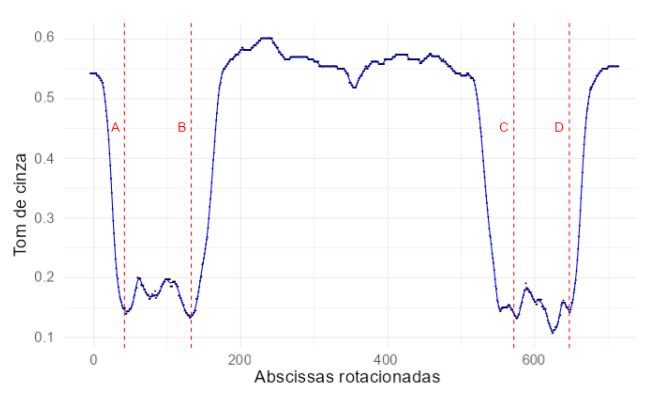
The process involved generating random values adhering to a bivariate normal distribution for the wheel markings, and the addition of a random error, also parametrized, to the temporal markings, followed by the assessment of the model over N Monte Carlo cycles. The resulting data was summarized with confidence-interval estimates for every output variable, based on positional measurements.

Figure 5 illustrates the procedure: two video frames were imported into Amped Five [24], aligned, and overlaid so that the vehicle's position at two distinct instants can be

viewed simultaneously. The figure also contains a scatter plot of the detected wheel-mark points and the orthogonal-regression line fitted to them.

The second workspace is designated for setting up the simulation parameters needed to estimate motion metrics based on the marked reference points.

The first input field controls the standard deviation (sd), of an isotropic Gaussian filter applied to the image prior to calculating the gray-tone transect along the orthogonal regression (Figure 6). This smoothing procedure reduces the influence of local pixel-level noise, producing a grayscale profile that is less affected by residual inconsistencies. In this case, distinct points associated with the centers of the wheels can be observed, validating the accuracy of the manually marked reference points.



**Figure 6.** Illustrative grayscale transect ("Tom de cinza") as a function of rotated abscissas ("Abscissas rotacionadas"), smoothed using an isotropic Gaussian filter (*s.d.* = 7) for orthogonal regression; red dashed lines mark the wheel reference points (A-D). Output generated by the application.

Next, input fields are shown for: timestamps for the reference frames, the known reference distance between wheel centers, the mean and standard deviation of timestamp errors (used to inject uncertainty into the simulated timing), the number of Monte Carlo repetitions, and the confidence level  $(1-\alpha)$  used to compute confidence intervals for the mean scalar-velocity. The corresponding distribution of estimates obtained from the simulation is summarized in Figure 7.

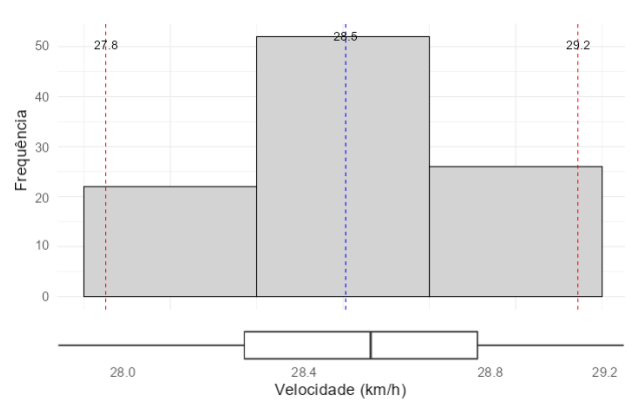
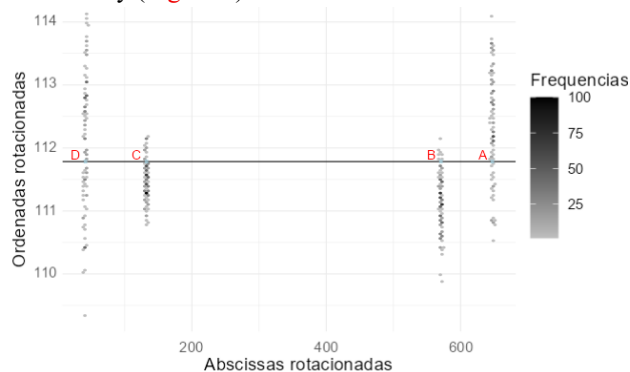


Figure 7. Example of nonparametric histogram with an overlaid box plot of mean scalar-velocity ("Velocidade") estimates. Dashed red lines mark

the 99% confidence interval; the dashed blue line marks the sample mean. Output generated by the application.

The simulations of the markings by the MCM, as well as the final orthogonal regression, are presented in a graph with axes rotated in order to align the regression line horizontally (Figure 8).



**Figure 8.** Illustrative scatter plot of rotated coordinates ("Abscissas rotacionadas" × "Ordenadas rotacionadas"), showing point densities from the MCM output. Grayscale point density reflects frequency of estimates; red labels (A–D) mark the projected centers of gravity for the reference points. Output generated by the application.

#### 3.1. Case study

To conduct the case study, a 1/10 scale Traxxas brand electric car, model 86086-4, was used (Figure 9). The choice of a scaled-down model was justified by increased safety, reduced risks, and lower operational costs. The vehicle was equipped with an odometer and real-time telemetry features, and its records were used as reference values.



Figure 9. Side view of the electric vehicle used (Image obtained from the manufacturer's website [25]).

Before the experiment, two chessboard-pattern templates, adjusted to the size of an A4 paper sheet, were placed on the ground (Figure 10). These templates were used for camera calibration and as a reference for estimating the distance traveled by the vehicle through conventional photogrammetry.

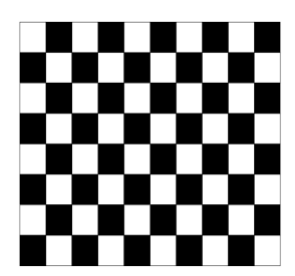


**Figure 10.** Reduced scale of the chessboard template used for photogrammetric estimation. The real one has 20x20mm squares.

The vehicle was operated to traverse a straight and flat road section at various speeds. A digital camera was set up on a tripod, positioned 1.5 meters from the vehicle's trajectory, at a 90° angle. The camera recorded at a rate of 30 frames per second (Figure 11).



Figure 11. Layout of the camera, tripod and chessboard templates.

The estimation of the camera's temporal marking error was based on the procedure outlined by SWGDE [26], using a Raspberry Pi Pico based device with two LEDs (Figure 12). A detailed description of the constructed device, its operation, and the developed code are available in a public repository<sup>2</sup>. A total of 19 videos, each approximately 10 minutes long, of the device operating were recorded by the camera used in the photogrammetric experiment.

To estimate the average error of the temporal markings of the video frames recorded by the camera, a 5-minute video at 30 fps was recorded, with two LEDs alternating their states every 10 seconds. The switching times were recorded by the Raspberry Pi Pico in a CSV file and matched with the temporal markings of the corresponding frames. The average estimated error for the temporal markings was 0.881 ms/s, with a standard deviation of 0.287 ms/s. The Kolmogorov-Smirnov test did not detect a significant difference between the obtained values' distribution and the normal distribution (p = 0.595). A histogram obtained through non-parametric bootstrap of the sample mean of these data with 10,000 repetitions is shown in Figure 13.

<sup>&</sup>lt;sup>2</sup> Available at https://github.com/demusis/calibrador\_tf.



**Figure 12.** Device setup used to estimate the average error in the temporal markings of the camera used.

The cross-ratio was calculated from 40 experimental repetitions, which were used to estimate the mean scalar speed using the developed application and Amped FIVE software. Scene calibration was performed using chessboard pattern templates and known distances to define the scale and correct for perspective. Afterwards, the vehicle's movement was tracked across the video. The application enabled the marking of the vehicle's position across multiple frames, while Amped FIVE used the vehicle's trajectory and the calibrated scene to calculate speed based on the tracked distance and corresponding time intervals.

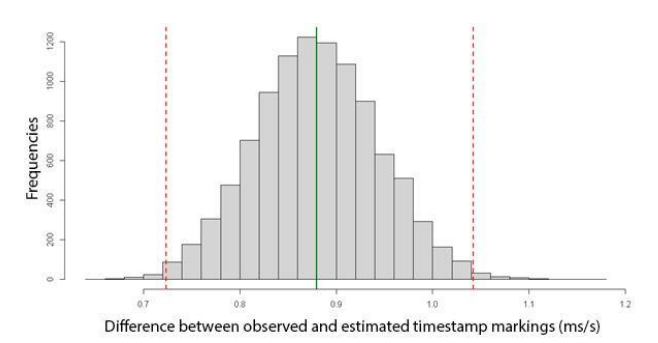


**Figure 13.** Non-parametric Bootstrap histogram of the average error in temporal markings of the camera used, with 99% confidence interval limits in dashed red and the sample mean in solid green.

Normality of the paired differences between the developed application and Amped FIVE results was assessed with the Kolmogorov–Smirnov test (p < 0.01), which indicated a significant deviation from normality, justifying the use of non-parametric methods. Accordingly, the two sets of estimates were compared with the Wilcoxon signed-rank test, which evaluates whether the median difference is zero without assuming normality. The test revealed no significative difference between methods (p = 0.722).

The mean absolute error was 0.0225 km/h, and a non-parametric bootstrap distribution based on 10,000 resamples is shown in Figure 14.

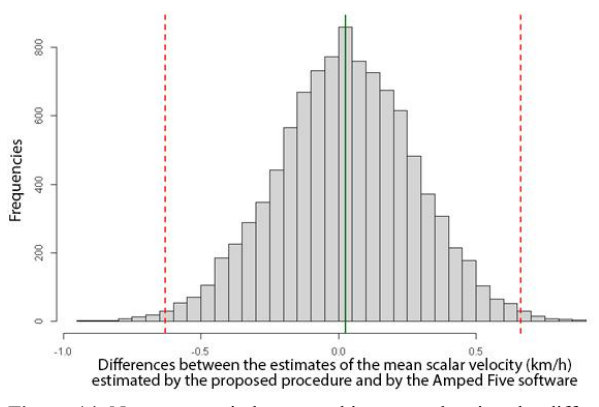


**Figure 14.** Non-parametric bootstrap histogram showing the difference between speed estimates from the developed application and Amped FIVE software, with 99% confidence interval limits in dashed red and the sample mean in solid green.

## 4. CONCLUSION

The developed software, by integrating the Monte Carlo method (MCM) and the concept of cross-ratio from projective geometry, provided a more precise and reliable analysis of the parameters involved in traffic accidents. By reconstructing the accidents in detail, the software contributes, in the Arendtian sense of "work" to the elucidation of factual truth.

Controlled experiments on a reduced scale, using a 1/10 scale electric car and high-precision cameras, validated the effectiveness of the methodology for estimating vehicle speeds from videos. The obtained estimates did not show statistically significant differences compared to those from the Amped FIVE software.

The cross-ratio has demonstrated its effectiveness as a tool within this context, and the integration of the MCM improved the analysis, allowing for the stochastic modeling of input variables, propagation of uncertainties, and providing probability distributions of the parameters of interest, resulting in a more robust and reliable analysis. Furthermore, the generation of confidence intervals by the MCM offers a measure of accuracy essential for forensic analyses.

The application developed in R language using the Shiny library provided a user-friendly graphical interface and web access, facilitating data entry, processing, and result visualization. The functionality for marking points on video frames, applying MCM, and visualizing speed estimates with associated confidence intervals made the process more accessible for forensic professionals.

The application has proven to be efficient in its operation and has the potential to contribute to experts and professionals in the field, highlighting the applicability and validity of the proposed approach for real traffic accident investigations. The integration of the MCM with the crossratio and the developed graphical interface presents a promising alternative for the reconstruction of traffic accidents.

## REFERENCES

- [1] M.F. Santos; N. P. Araujo. Perfil sociodemográfico das vítimas de acidentes de trânsito no Estado de Roraima. *Health and Diversity (Online)*, Boa Vista, Brazil, 1: 71-77 (2017).
- [2] N.M. Zanon; L. F. R. Brisotto. Comportamento de risco e a contribuição da psicologia para a redução dos acidentes de trânsito: uma revisão da literatura. *Revista Destaques Acadêmicos*, Lajeado, RS, Brazil, **12**(2): 23-41 (2020).
- [3] G.C. Massaú; R. G. Rosa. Acidentes de trânsito e direito à saúde: prevenção de vidas e economia pública. *Revista de Direito Sanitário*, São Paulo, Brazil, **17**(2): 30-47 (2016).
- [4] L.V. Ramos; I.C. Barreto; F.B. Miguel. Morbimortalidade por acidentes de trânsito terrestres na Bahia entre os anos de 2011 e 2021. *Rev. Ciênc. Méd. Biol.*, Salvador, Brazil, **21**(3): 593-604 (2022).
- [5] H. Arendt. *A condição humana*. Translator: Roberto Raposo. 13. ed. Rio de Janeiro: Forense Universitária, (2016) 474p.
- [6] D.P. Landau; K. Binder. *A guide to Monte Carlo simulations in statistical physics*. 5. ed. Cambridge: Cambridge University Press (2021) 582p.
- [7] T.W. Wong; C.H. Tao; Y.K. Cheng; K.H. Wong; C.N. Tam. Application of cross-ratio in traffic accident reconstruction. *Forensic Science International* **235**: 19–23 (2013).
- [8] A. Koranyi; H.M. Riemann. Foundations of the theory in quasiconformal mappings on the Heisenberg group. *Advances in Math* **111**(1): 1–87 (1995).
- [9] B.M. Ayyub; G.J. Klir. *Uncertainty modeling and analysis in engineering and the sciences*. 1. ed. Boca Raton, US: Chapman & Hall/CRC (2006) 400p.
- [10] M. Rausand; A. Høyland. *System reliability theory: models, statistical methods, and applications.* 3<sup>a</sup>. ed. New Jersey, US: John Wiley & Sons (2020) 864p.
- [11] C.P. Robert; G. Casella. *Monte Carlo statistical methods*. 2ª ed. New York: Springer (2010) 649p.
- [12] D.P. Kroese; T. Brereton; T. Taimre; Z. Botev. Why the Monte Carlo method is so important today. *WIREs Computational Statistics*, **6**: 386-392 (2014).
- [13] C.M. Bishop. *Pattern recognition and machine learning*. New York: Springer (2011) 738p.
- [14] A. Gelman; J.B. Carlin; H.S. Stern. *Bayesian data analysis*. 3<sup>a</sup> ed. Boca Raton, US: Chapman & Hall/CRC, (2013) 675p.
- [15] R.Y. Rubinstein; D. P. Kroese. *Simulation and the Monte Carlo method*. 3<sup>a</sup> ed. New Jersey, US: John Wiley & Sons (2016) 432p.
- [16] J.A. Doornik; H. Hansen. An Omnibus test for univariate and multivariate normality. *Oxford Bulletin of Economics and Statistics*, Oxford, England, **70**: 927-939 (2008).

- [17] H. Akaike. A new look at the statistical model identification. *IEEE Transactions on Automatic Control* **19**(6): 716-723 (1974).
- [18] K.P. Burnham; D. R. Anderson. Multimodel inference: understanding AIC and BIC in model selection. *Sociological methods & research* **33**(2): 261-304 (2004).
- [19] T. Gross. *Laudo pericial 2.12.2022.50271-01*. Mato Grosso, Brazil: Perícia Oficial e Identificação Técnica do Estado de Mato Grosso (POLITEC/MT), 2022. Available at: https://portal2.sesp.mt.gov.br/atena/. Accessed at: Dec 19, 2024.
- [20] R Core Team. R: A Language and Environment for Statistical Computing. Version 4.4.0. Vienna, Austria: R Foundation for Statistical Computing, 2024. Available at: https://www.r-project.org/. Accessed at: Dec. 19, 2024.
- [21] Posit Team. *RStudio: Integrated Development Environment for R.* Version 2024.12.0. Boston, MA: Posit Software, PBC, 2024. Available at: http://www.posit.co/. Accessed at: Dec. 18, 2024.
- [22] W. Chang; J. Cheng; J.J. Allaire; C. Sievert; B. Schloerke; Y. Xie; J. Allen; J. Mcpherson; A. Dipert; B. Borges. *Shiny: Web Application Framework for R*. Version 1.8.1.1, 2024. Available at: https://CRAN.R-project.org/package=shiny. Accessed at: Dec. 11, 2024.
- [23] The Bootstrap Authors. *Bootstrap*. Version 5.3.3, 2024. Available at: https://getbootstrap.com/. Accessed at: Jun. 7, 2024.
- [24] AMPED Software. *Amped FIVE*. 2024. Available at: https://ampedsoftware.com/five. Accessed at: May 9, 2024.
- [25] Traxxas. *Traxxas: The Fastest Name in Radio Control*. McKinney, Texas, 2024. Available at: https://traxxas.com/. Accessed at: Dec. 7, 2024.
- [26] Scientific Working Group on Digital Evidence (SWGDE). SWGDE Best Practices for Frame Timing Analysis of Video Stored in ISSO Base Media File Formats. Version 1.1 (June 9, 2022). Available at: https://www.swgde.org/19-v-004/. Accessed at: Apr. 21, 2024.